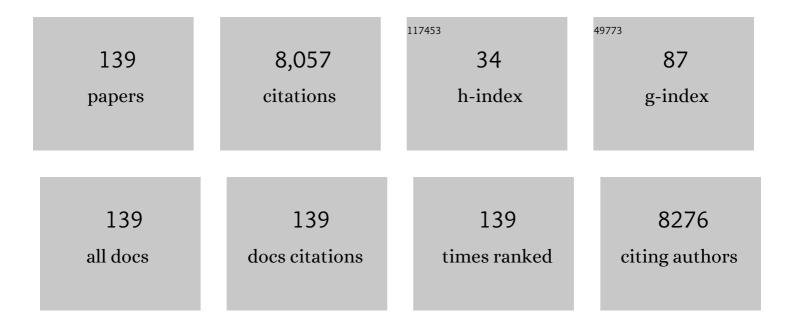
Choonsik Lee

List of Publications by Year in descending order

Source: https://exaly.com/author-pdf/9235464/publications.pdf Version: 2024-02-01



#	Article	IF	CITATIONS
1	Development of whole-body representation and dose calculation in a commercial treatment planning system. Zeitschrift Fur Medizinische Physik, 2022, 32, 159-172.	0.6	4
2	Japanese pediatric and adult atomic bomb survivor dosimetry: potential improvements using the J45 phantom series and modern Monte Carlo transport. Radiation and Environmental Biophysics, 2022, 61, 73-86.	0.6	5
3	Association Between Radioactive Iodine Treatment for Pediatric and Young Adulthood Differentiated Thyroid Cancer and Risk of Second Primary Malignancies. Journal of Clinical Oncology, 2022, 40, 1439-1449.	0.8	45
4	Fetal dose from proton pencil beam scanning craniospinal irradiation during pregnancy: a Monte Carlo study. Physics in Medicine and Biology, 2022, 67, 035003.	1.6	5
5	Body region-specific 3D age-scaling functions for scaling whole-body computed tomography anatomy for pediatric late effects studies. Biomedical Physics and Engineering Express, 2022, 8, 025010.	0.6	0
6	Childhood cancer risks estimates following CT scans: an update of the French CT cohort study. European Radiology, 2022, 32, 5491-5498.	2.3	17
7	Specific absorbed fractions for a revised series of the UF/NCI pediatric reference phantoms: internal photon sources. Physics in Medicine and Biology, 2021, 66, 035006.	1.6	8
8	Specific absorbed fractions for a revised series of the UF/NCI pediatric reference phantoms: internal electron sources. Physics in Medicine and Biology, 2021, 66, 035005.	1.6	6
9	Fluoroscopy X-Ray Organ-Specific Dosimetry System (FLUXOR) for Estimation of Organ Doses and Their Uncertainties in the Canadian Fluoroscopy Cohort Study. Radiation Research, 2021, 195, 385-396.	0.7	1
10	Dose quantities for measurement and comparison of doses to individual patients in computed tomography (CT). Journal of Radiological Protection, 2021, 41, .	0.6	1
11	Dose conversion coefficients for neutron external exposures with five postures: walking, sitting, bending, kneeling, and squatting. Radiation and Environmental Biophysics, 2021, 60, 317-328.	0.6	3
12	Managing Radiation Dose from Chest CT in Patients with COVID-19. Radiology, 2021, 298, E158-E159.	3.6	17
13	Dose Estimation for the European Epidemiological Study on Pediatric Computed Tomography (EPI-CT). Radiation Research, 2021, 196, 74-99.	0.7	17
14	Conversion factors to derive organ doses for canine subjects undergoing CT examinations. Veterinary Radiology and Ultrasound, 2021, 62, 421-428.	0.4	0
15	Lymphoma and multiple myeloma in cohorts of persons exposed to ionising radiation at a young age. Leukemia, 2021, 35, 2906-2916.	3.3	7
16	Application of an automatic segmentation method for evaluating cardiac structure doses received by breast radiotherapy patients. Physics and Imaging in Radiation Oncology, 2021, 19, 138-144.	1.2	8
17	Trends in Occupational Radiation Doses for U.S. Radiologic Technologists Performing General Radiologic and Nuclear Medicine Procedures, 1980–2015. Radiology, 2021, 300, 605-612.	3.6	13
18	Extensive study of radiation dose on human body at aviation altitude through Monte Carlo simulation. Life Sciences in Space Research, 2021, 31, 1-13.	1.2	1

#	Article	IF	CITATIONS
19	A Monte Carlo model for organ dose reconstruction of patients in pencil beam scanning (PBS) proton therapy for epidemiologic studies of late effects. Journal of Radiological Protection, 2020, 40, 225-242.	0.6	12
20	Dose coefficients of percentile-specific computational phantoms for photon external exposures. Radiation and Environmental Biophysics, 2020, 59, 151-160.	0.6	6
21	Organ Doses from Chest Radiographs in Tuberculosis Patients in Canada and Their Uncertainties in Periods from 1930 to 1969. Health Physics, 2020, 119, 176-191.	0.3	1
22	Fabrication of a pediatric torso phantom with multiple tissues represented using a dual nozzle thermoplastic 3D printer. Journal of Applied Clinical Medical Physics, 2020, 21, 226-236.	0.8	11
23	NCINM: organ dose calculator for patients undergoing nuclear medicine procedures. Biomedical Physics and Engineering Express, 2020, 6, 055010.	0.6	7
24	Cancer therapy shapes the fitness landscape of clonal hematopoiesis. Nature Genetics, 2020, 52, 1219-1226.	9.4	367
25	Development and validation of an age-scalable cardiac model with substructures for dosimetry in late-effects studies of childhood cancer survivors. Radiotherapy and Oncology, 2020, 153, 163-171.	0.3	7
26	INVESTIGATION OF THE INFLUENCE OF THYROID LOCATION ON IODINE-131ÂS VALUES. Radiation Protection Dosimetry, 2020, 189, 163-171.	0.4	5
27	Patient radiation dose from x-ray guided endovascular aneurysm repair: a Monte Carlo approach using voxel phantoms and detailed exposure information. Journal of Radiological Protection, 2020, 40, 704-726.	0.6	17
28	Adult patient-specific CT organ dose estimations using automated segmentations and Monte Carlo simulations. Biomedical Physics and Engineering Express, 2020, 6, 045016.	0.6	4
29	How to estimate effective dose for CT patients. European Radiology, 2020, 30, 1825-1827.	2.3	15
30	The HARMONIC project: Study design for assessment of cancer risks following cardiac fluoroscopy in childhood. Journal of Radiological Protection, 2020, , .	0.6	6
31	CT DOSIMETRY FOR THE AUSTRALIAN COHORT DATA LINKAGE STUDY. Radiation Protection Dosimetry, 2020, 191, 423-438.	0.4	4
32	Dosimetric Impact of a New Computational Voxel Phantom Series for the Japanese Atomic Bomb Survivors: Methodological Improvements and Organ Dose Response Functions. Radiation Research, 2020, 194, 390-402.	0.7	5
33	Radiation Exposure From Pediatric CT Scans and Subsequent Cancer Risk in the Netherlands. Journal of the National Cancer Institute, 2019, 111, 256-263.	3.0	218
34	A Feasibility Study to Reduce Misclassification Error in Occupational Dose Estimates for Epidemiological Studies Using Body Size-Dependent Computational Phantoms. IEEE Transactions on Radiation and Plasma Medical Sciences, 2019, 3, 83-88.	2.7	4
35	Dosimetric impact of voxel resolutions of computational human phantoms for external photon exposure. Biomedical Physics and Engineering Express, 2019, 5, 065002.	0.6	2
36	Conversion of computational human phantoms into DICOM-RT for normal tissue dose assessment in radiotherapy patients. Physics in Medicine and Biology, 2019, 64, 13NT02.	1.6	11

#	Article	IF	CITATIONS
37	S VALUES FOR NEUROIMAGING PROCEDURES ON KOREAN PEDIATRIC AND ADULT HEAD COMPUTATIONAL PHANTOMS. Radiation Protection Dosimetry, 2019, 185, 168-175.	0.4	4
38	Dosimetric Impact of a New Computational Voxel Phantom Series for the Japanese Atomic Bomb Survivors: Pregnant Females. Radiation Research, 2019, 192, 538.	0.7	14
39	Automatic segmentation of cardiac structures for breast cancer radiotherapy. Physics and Imaging in Radiation Oncology, 2019, 12, 44-48.	1.2	18
40	Pragmatic randomised clinical trial of proton versus photon therapy for patients with non-metastatic breast cancer: the Radiotherapy Comparative Effectiveness (RadComp) Consortium trial protocol. BMJ Open, 2019, 9, e025556.	0.8	60
41	Automatic Mapping of CT Scan Locations on Computational Human Phantoms for Organ Dose Estimation. Journal of Digital Imaging, 2019, 32, 175-182.	1.6	4
42	Patterns of proton therapy use in pediatric cancer management in 2016: An international survey. Radiotherapy and Oncology, 2019, 132, 155-161.	0.3	42
43	ORGAN DOSE ESTIMATION ACCOUNTING FOR UNCERTAINTY FOR PEDIATRIC AND YOUNG ADULT CT SCANS IN THE UNITED KINGDOM. Radiation Protection Dosimetry, 2019, 184, 44-53.	0.4	9
44	Organ doses evaluation for chest computed tomography procedures with TL dosimeters: Comparison with Monte Carlo simulations. Journal of Applied Clinical Medical Physics, 2019, 20, 308-320.	0.8	32
45	Cumulative Radiation Exposures from CT Screening and Surveillance Strategies for von Hippel-Lindau–associated Solid Pancreatic Tumors. Radiology, 2019, 290, 116-124.	3.6	7
46	Dosimetric Impact of a New Computational Voxel Phantom Series for the Japanese Atomic Bomb Survivors: Children and Adults. Radiation Research, 2019, 191, 369.	0.7	17
47	Suggestion of reduced cancer risks following cardiac x-ray exposures is unconvincing. European Journal of Epidemiology, 2018, 33, 427-428.	2.5	2
48	Cancer incidence among children and young adults who have undergone x-ray guided cardiac catheterization procedures. European Journal of Epidemiology, 2018, 33, 393-401.	2.5	26
49	ESTIMATION OF ORGAN DOSES AMONG DIAGNOSTIC MEDICAL RADIATION WORKERS IN SOUTH KOREA. Radiation Protection Dosimetry, 2018, 179, 142-150.	0.4	12
50	Lens Dose Reduction by Patient Posture Modification During Neck CT. American Journal of Roentgenology, 2018, 210, 1111-1117.	1.0	11
51	A NOVEL METHOD TO ESTIMATE LYMPHOCYTE DOSE AND APPLICATION TO PEDIATRIC AND YOUNG ADULT CT PATIENTS IN THE UNITED KINGDOM. Radiation Protection Dosimetry, 2018, 178, 116-121.	0.4	6
52	Individual radiation exposure from computed tomography: a survey of paediatric practice in French university hospitals, 2010–2013. European Radiology, 2018, 28, 630-641.	2.3	15
53	Body-weight dependent dose coefficients for adults exposed to idealised external photon fields. Journal of Radiological Protection, 2018, 38, 1441-1453.	0.6	4
54	A Novel Method to Extend a Partial-Body CT for the Reconstruction of Dose to Organs beyond the Scan Range. Radiation Research, 2018, 189, 618-626.	0.7	9

#	Article	IF	CITATIONS
55	Disparities in Radiation Burden from Trauma Evaluation at Pediatric Versus Nonpediatric Institutions. Journal of Surgical Research, 2018, 232, 475-483.	0.8	5
56	Subtle excess in lifetime cancer risk related to CT scanning in Spanish young people. Environment International, 2018, 120, 1-10.	4.8	15
57	Suggested reference values for regional blood volumes in children and adolescents. Physics in Medicine and Biology, 2018, 63, 155022.	1.6	19
58	Leukaemia and myeloid malignancy among people exposed to low doses (<100 mSv) of ionising radiation during childhood: a pooled analysis of nine historical cohort studies. Lancet Haematology,the, 2018, 5, e346-e358.	2.2	103
59	Feasibility and accuracy of UF/NCI phantoms and Monte Carlo retrospective dosimetry in children treated on National Wilms Tumor Study protocols. Pediatric Blood and Cancer, 2018, 65, e27395.	0.8	6
60	Patient characteristics associated with differences in radiation exposure from pediatric abdomen-pelvis CT scans: a quantile regression analysis. Computers in Biology and Medicine, 2017, 85, 7-12.	3.9	10
61	Body Size–Specific Organ and Effective Doses of Chest CT Screening Examinations of the National Lung Screening Trial. American Journal of Roentgenology, 2017, 208, 1082-1088.	1.0	18
62	How to identify high radiation burden from computed tomography: an example in obese children. Journal of Surgical Research, 2017, 217, 54-62.e3.	0.8	1
63	Simulation study of personal dose equivalent for external exposure to radioactive cesium distributed in soil. Journal of Nuclear Science and Technology, 2017, 54, 1018-1027.	0.7	10
64	Projected cancer risks potentially related to past, current, and future practices in paediatric CT in the United Kingdom, 1990–2020. British Journal of Cancer, 2017, 116, 109-116.	2.9	40
65	KOREAN PEDIATRIC AND ADULT HEAD COMPUTATIONAL PHANTOMS AND APPLICATION TO PHOTON SPECIFIC ABSORBED FRACTIONS CALCULATIONS. Radiation Protection Dosimetry, 2017, 176, 294-301.	0.4	6
66	A Review of Radiotherapy-Induced Late Effects Research after Advanced Technology Treatments. Frontiers in Oncology, 2016, 6, 13.	1.3	67
67	<i>S</i> values for ¹³¹ I based on the ICRP adult voxel phantoms. Radiation Protection Dosimetry, 2016, 168, 92-110.	0.4	20
68	Reconstruction of paediatric organ doses from axial CT scans performed in the 1990s – range of doses as input to uncertainty estimates. European Radiology, 2016, 26, 3026-3033.	2.3	5
69	BODY SIZE-SPECIFIC EFFECTIVE DOSE CONVERSION COEFFICIENTS FOR CT SCANS. Radiation Protection Dosimetry, 2016, 172, 428-437.	0.4	32
70	Reduction in radiation doses from paediatric CT scans in Great Britain. British Journal of Radiology, 2016, 89, 20150305.	1.0	32
71	Age-dependent dose conversion coefficients for external exposure to radioactive cesium in soil. Journal of Nuclear Science and Technology, 2016, 53, 69-81.	0.7	23
72	Incorporation of detailed eye model into polygon-mesh versions of ICRP-110 reference phantoms. Physics in Medicine and Biology, 2015, 60, 8695-8707.	1.6	29

#	Article	IF	CITATIONS
73	NCICT: a computational solution to estimate organ doses for pediatric and adult patients undergoing CT scans. Journal of Radiological Protection, 2015, 35, 891-909.	0.6	123
74	Effective dose conversion coefficients for health care provider exposed to pediatric and adult victims in radiological dispersal device incident. Journal of Radiological Protection, 2015, 35, 37-45.	0.6	6
75	Reconstruction of organ dose for external radiotherapy patients in retrospective epidemiologic studies. Physics in Medicine and Biology, 2015, 60, 2309-2324.	1.6	27
76	Assessment of radiation dose in nuclear cardiovascular imaging using realistic computational models. Medical Physics, 2015, 42, 2955-2966.	1.6	6
77	Calculation of Organ Doses for a Large Number of Patients Undergoing CT Examinations. American Journal of Roentgenology, 2015, 205, 827-833.	1.0	12
78	Patient-Specific Dosimetry Using Pretherapy [124I]m-iodobenzylguanidine ([124I]mIBG) Dynamic PET/CT Imaging Before [131I]mIBG Targeted Radionuclide Therapy for Neuroblastoma. Molecular Imaging and Biology, 2015, 17, 284-294.	1.3	67
79	Organ and effective dose conversion coefficients for a sitting female hybrid computational phantom exposed to monoenergetic protons in idealized irradiation geometries. Physics in Medicine and Biology, 2014, 59, 7957-8003.	1.6	8
80	The UF/NCI family of hybrid computational phantoms representing the current US population of male and female children, adolescents, and adults—application to CT dosimetry. Physics in Medicine and Biology, 2014, 59, 5225-5242.	1.6	99
81	Nuclear Medicine Practices in the 1950s through the Mid-1970s and Occupational Radiation Doses to Technologists from Diagnostic Radioisotope Procedures. Health Physics, 2014, 107, 300-310.	0.3	10
82	A practical guideline for the release of patients treated by I-131 based on Monte Carlo dose calculations for family members. Journal of Radiological Protection, 2014, 34, N7-N17.	0.6	7
83	Leukemia and brain tumors among children after radiation exposure from CT scans: design and methodological opportunities of the Dutch Pediatric CT Study. European Journal of Epidemiology, 2014, 29, 293-301.	2.5	40
84	Personalized Technologist Dose Audit Feedback for Reducing Patient Radiation Exposure From CT. Journal of the American College of Radiology, 2014, 11, 300-308.	0.9	15
85	Database of normalised computed tomography dose index for retrospective CT dosimetry. Journal of Radiological Protection, 2014, 34, 363-388.	0.6	17
86	Monte Carlo simulations of adult and pediatric computed tomography exams: Validation studies of organ doses with physical phantoms. Medical Physics, 2013, 40, 013901.	1.6	52
87	Prediction of the location and size of the stomach using patient characteristics for retrospective radiation dose estimation following radiotherapy. Physics in Medicine and Biology, 2013, 58, 8739-8753.	1.6	11
88	Organ S values and effective doses for family members exposed to adult patients following I-131 treatment: A Monte Carlo simulation study. Medical Physics, 2013, 40, 083901.	1.6	13
89	Evaluation of the use of surrogate tissues for calculating radiation dose to lymphatic nodes from external photon beams. Radiation Protection Dosimetry, 2013, 157, 600-609.	0.4	0
90	TEDE per cumulated activity for family members exposed to adult patients treated with 131I. Radiation Protection Dosimetry, 2013, 153, 448-456.	0.4	3

#	Article	IF	CITATIONS
91	Computational lymphatic node models in pediatric and adult hybrid phantoms for radiation dosimetry. Physics in Medicine and Biology, 2013, 58, N59-N82.	1.6	26
92	Influence of eye size and beam entry angle on dose to non-targeted tissues of the eye during stereotactic x-ray radiosurgery of AMD. Physics in Medicine and Biology, 2013, 58, 6887-6896.	1.6	10
93	Pediatric radiation dosimetry for positronâ€emitting radionuclides using anthropomorphic phantoms. Medical Physics, 2013, 40, 102502.	1.6	22
94	Assessing Organ Doses from Paediatric CT Scans—A Novel Approach for an Epidemiology Study (the) Tj ETQq0	0 0 rgBT /(1.2	Overlock 10 32
95	CT Scans in Young People in Great Britain: Temporal and Descriptive Patterns, 1993–2002. Radiology Research and Practice, 2012, 2012, 1-8.	0.6	29
96	Organ doses for reference pediatric and adolescent patients undergoing computed tomography estimated by Monte Carlo simulation. Medical Physics, 2012, 39, 2129-2146.	1.6	93
97	GUIDANCE ON THE USE OF HANDHELD SURVEY METERS FOR RADIOLOGICAL TRIAGE. Health Physics, 2012, 102, 305-325.	0.3	15
98	HYBRID COMPUTATIONAL PHANTOMS REPRESENTING THE REFERENCE ADULT MALE AND ADULT FEMALE. Health Physics, 2012, 102, 292-304.	0.3	29
99	Use of Diagnostic Imaging Studies and Associated Radiation Exposure for Patients Enrolled in Large Integrated Health Care Systems, 1996-2010. JAMA - Journal of the American Medical Association, 2012, 307, 2400-9.	3.8	685
100	Internal photon and electron dosimetry of the newborn patient—a hybrid computational phantom study. Physics in Medicine and Biology, 2012, 57, 1433-1457.	1.6	20
101	Radiation exposure from CT scans in childhood and subsequent risk of leukaemia and brain tumours: a retrospective cohort study. Lancet, The, 2012, 380, 499-505.	6.3	3,011
102	Cancer risks associated with external radiation from diagnostic imaging procedures. Ca-A Cancer Journal for Clinicians, 2012, 62, 75-100.	157.7	287
103	Evolving Strategies in Epidemiologic Research on Radiation and Cancer. Radiation Research, 2011, 176, 527-532.	0.7	2
104	Comparison of internal dosimetry factors for three classes of adult computational phantoms with emphasis on I-131 in the thyroid. Physics in Medicine and Biology, 2011, 56, 7317-7335.	1.6	34
105	Organ doses for reference adult male and female undergoing computed tomography estimated by Monte Carlo simulations. Medical Physics, 2011, 38, 1196-1206.	1.6	81
106	An image-based skeletal dosimetry model for the ICRP reference adult male—internal electron sources. Physics in Medicine and Biology, 2011, 56, 2309-2346.	1.6	76
107	Response functions for computing absorbed dose to skeletal tissues from photon irradiation—an update. Physics in Medicine and Biology, 2011, 56, 2347-2365.	1.6	77
108	Hybrid computational phantoms for medical dose reconstruction. Radiation and Environmental Biophysics, 2010, 49, 155-168.	0.6	54

#	Article	IF	CITATIONS
109	Hybrid computational phantoms for medical dose reconstruction: Response to Kramer and Cassola. Radiation and Environmental Biophysics, 2010, 49, 501-502.	0.6	0
110	An image-based skeletal dosimetry model for the ICRP reference newborn—internal electron sources. Physics in Medicine and Biology, 2010, 55, 1785-1814.	1.6	23
111	The UF family of reference hybrid phantoms for computational radiation dosimetry. Physics in Medicine and Biology, 2010, 55, 339-363.	1.6	277
112	SAR calculations from 20 MHz to 6 GHz in the University of Florida newborn voxel phantom and their implications for dosimetry. Physics in Medicine and Biology, 2010, 55, 1519-1530.	1.6	32
113	Kilovoltage stereotactic radiosurgery for age-related macular degeneration: Assessment of optic nerve dose and patient effective dose. Medical Physics, 2009, 36, 3671-3681.	1.6	33
114	The influence of patient size on dose conversion coefficients: a hybrid phantom study for adult cardiac catheterization. Physics in Medicine and Biology, 2009, 54, 3613-3629.	1.6	39
115	An image-based skeletal tissue model for the ICRP reference newborn. Physics in Medicine and Biology, 2009, 54, 4497-4531.	1.6	25
116	An Algorithm for Lymphatic Node Placement in Hybrid Computational Phantoms—Applications to Radionuclide Therapy Dosimetry. Proceedings of the IEEE, 2009, 97, 2098-2108.	16.4	6
117	Hybrid Patient-Dependent Phantoms Covering Statistical Distributions of Body Morphometry in the U.S. Adult and Pediatric Population. Proceedings of the IEEE, 2009, 97, 2060-2075.	16.4	38
118	Development of Deformable Computational Model for Korean Adult Male Based on Polygon and NURBS Surfaces. Nuclear Technology, 2009, 168, 227-230.	0.7	0
119	Organ Absorbed Doses and Effective Doses to the Patient and the Medical Staff in Interventional Radiology Calculated from Voxel Phantom. Journal of Nuclear Science and Technology, 2008, 45, 309-312.	0.7	0
120	Hybrid computational phantoms of the 15â€year male and female adolescent: Applications to CT organ dosimetry for patients of variable morphometry. Medical Physics, 2008, 35, 2366-2382.	1.6	70
121	HDRK-Man: a whole-body voxel model based on high-resolution color slice images of a Korean adult male cadaver. Physics in Medicine and Biology, 2008, 53, 4093-4106.	1.6	76
122	Anthropometric approaches and their uncertainties to assigning computational phantoms to individual patients in pediatric dosimetry studies. Physics in Medicine and Biology, 2008, 53, 453-471.	1.6	20
123	Dosimetry characterization of a multibeam radiotherapy treatment for ageâ€related macular degeneration. Medical Physics, 2008, 35, 5151-5160.	1.6	29
124	Consideration of the ICRP 2006 revised tissue weighting factors on age-dependent values of the effective dose for external photons. Physics in Medicine and Biology, 2007, 52, 41-58.	1.6	17
125	Organ and effective doses in pediatric patients undergoing helical multislice computed tomography examination. Medical Physics, 2007, 34, 1858-1873.	1.6	63
126	NURBS-based 3-d anthropomorphic computational phantoms for radiation dosimetry applications. Radiation Protection Dosimetry, 2007, 127, 227-232.	0.4	35

#	Article	IF	CITATIONS
127	Hybrid computational phantoms of the male and female newborn patient: NURBS-based whole-body models. Physics in Medicine and Biology, 2007, 52, 3309-3333.	1.6	164
128	Applicability of dose conversion coefficients of ICRP 74 to Asian adult males: Monte Carlo simulation study. Applied Radiation and Isotopes, 2007, 65, 593-598.	0.7	10
129	An assessment of bone marrow and bone endosteum dosimetry methods for photon sources. Physics in Medicine and Biology, 2006, 51, 5391-5407.	1.6	50
130	Development of the two Korean adult tomographic computational phantoms for organ dosimetry. Medical Physics, 2006, 33, 380-390.	1.6	76
131	Organ and effective doses in newborn patients during helical multislice computed tomography examination. Physics in Medicine and Biology, 2006, 51, 5151-5166.	1.6	29
132	Age-dependent organ and effective dose coefficients for external photons: a comparison of stylized and voxel-based paediatric phantoms. Physics in Medicine and Biology, 2006, 51, 4663-4688.	1.6	29
133	On the need to revise the arm structure in stylized anthropomorphic phantoms in lateral photon irradiation geometry. Physics in Medicine and Biology, 2006, 51, N393-N402.	1.6	6
134	Whole-body voxel phantoms of paediatric patients—UF Series B. Physics in Medicine and Biology, 2006, 51, 4649-4661.	1.6	77
135	The UF series of tomographic computational phantoms of pediatric patients. Medical Physics, 2005, 32, 3537-3548.	1.6	92
136	The effect of unrealistic thyroid vertical position on thyroid dose in the MIRD phantom. Medical Physics, 2004, 31, 2038-2041.	1.6	8
137	Korean adult male voxel model KORMAN segmented from magnetic resonance images. Medical Physics, 2004, 31, 1017-1022.	1.6	39
138	Implementation of Japanese Male and Female Tomographic Phantoms to Multi-particle Monte Carlo Code for Ionizing Radiation Dosimetry. , 0, .		2
139	Reply to P. Petranović OvÄariÄek et al. Journal of Clinical Oncology, 0, , .	0.8	0